Materials Science & Engineering A 632 (2015) 120–126

Contents lists available at ScienceDirect

Materials Science & Engineering A

journal homepage: www.elsevier.com/locate/msea

Rapid communication

# Variation of work hardening rate by oxygen contents in pure titanium alloy

Duck-soo Kang [a,b], Kwang-jin Lee [a,*], Eui-pyo Kwon [a], Toshihiro Tsuchiyama [b,c], Setsuo Takaki [b,c]

[a] Convergence Components & Agricultural Machinery Application Center, Korea Institute of Industrial Technology (KITECH), 838-11, Palbok-dong, Deokjin-gu, Jeonju-City 561-202, South Korea
[b] Department of Materials Science and Engineering, Kyushu University, 744 Motooka, Nishi-ku, Fukuoka 819-0395, Japan
[c] International Institute for Carbon Neutral Energy Research (WPI-I2CNER), Kyushu University, 744 Mooto-oka, Nishi-ku, Fukuoka 819-0395, Japan

ARTICLE INFO

*Article history:*
Received 13 January 2015
Accepted 26 February 2015
Available online 5 March 2015

*Keywords:*
Oxygen
Work hardening rate
Deformation behavior
Pure titanium alloy

ABSTRACT

Pure titanium–oxygen alloys with different oxygen contents were tensile-tested to investigate the effect of oxygen on work hardening rate and deformation behavior. Yield and ultimate tensile strengths markedly increased with increasing oxygen contents, although the elongations were decreased. Work hardening rate was also enhanced with increasing oxygen contents resulting in increase in the uniform elongation. The improved work hardening rate was ascribed to transition of primary deformation mode from twin deformation to dislocation slip by oxygen addition. When twin deformation is suppressed by oxygen addition, however, the $\langle c+a\rangle$ dislocation must function as a substitute for twinning to permit the homogeneous plastic deformation. It contributed that the improved work hardening rate without deformation twinning is thought to be a restriction of dislocation slips to a certain special plane by oxygen addition.



## 1. Introduction

Interstitial elements such as carbon, nitrogen and oxygen are well-known solid-solution strengtheners in titanium alloys. Especially, oxygen is widely used in commercial pure Ti and Ti alloys to obtain good mechanical properties [1]. For example, while grade 5 Ti–6Al–4V alloy with high oxygen content of 2000 ppm exhibits superior mechanical properties, grade 1 commercially pure Ti (CP Ti) has the lowest ultimate tensile strength among Ti alloys due to the lowest oxygen concentration. In particular, oxygen contents need to be carefully controlled to obtain optimal balance between strength and ductility [2].

It is well known that the *hcp*-structure CP Ti has an axial ratio of $c/a=1.587$, which is strongly plastically anisotropic. Furthermore, the $c/a$ ratio increases with oxygen concentrations. The mechanical response of *hcp* materials is strongly dependent on the combination of active deformation modes, which is affected by $c/a$ ratio [3]. The most common slip modes, in the order of ease of operation, are the $\{10\bar{1}0\}$, $\{10\bar{1}1\}$ and $\{0001\}$ planes, with $\langle 11\bar{2}0\rangle$ as the slip direction, that constitute a total of four independent slip systems [4]. However, five independent slip systems are necessary for the polycrystalline material to undergo general homogeneous plastic deformation. Thus, twin deformations are operated in order to maintain the deformation compatibility [5]. Hence, twin and slip deformations occur concomitantly during plastic deformation [6].

Oh et al. [7] studied the effect of oxygen content on the mechanical properties and lattice parameter of Ti–6Al–4V and CP Ti alloy. If the change in ultimate tensile strength is compared between these two alloys, it is clear that both exhibit a similar gradient with respect to oxygen concentration. Also, the lattice parameter $c/a$ ratio increased with oxygen concentration at a rate dependent on the alloy. It is thought that the change in lattice strain with respect to the interstitial concentration affects the mechanical properties, *i.e.* as both the $a$ and $c$ lattice parameters increase with increasing oxygen concentration, they begin to limit the number of slip planes and improve the strength, but at the same time limit the ductility of the alloy.

Although the mechanical properties and deformation behavior in *hcp* α-Ti alloys with various oxygen contents have been widely reported [8–10], precise influence of oxygen on the work hardening rate is not yet fully investigated.

In this study, various oxygen content was added to a pure Ti alloy to clarify the effect of oxygen on the work hardening rate. In particular, the variation of the work hardening rate by oxygen concentrations was discussed in terms of lattice parameter and deformed microstructures.

* Corresponding author. Fax: +82 632103700.
*E-mail address:* kjlee@kitech.re.kr (K.-j. Lee).

http://dx.doi.org/10.1016/j.msea.2015.02.074
0921-5093/

## 2. Experimental procedure

Table 1 shows the chemical compositions of the alloys used. All alloys containing oxygen (0.082–0.268 mass%) were prepared by a crucible levitation melting furnace. The oxygen contents were controlled by the appropriate addition of $TiO_2$ during melting. The α single-phase Ti–O alloys were hot-rolled in α and β single-phase regions, and after annealing the α single-phase region, were cold-rolled to a size of 800 × 300 × 5 (mm). After that, these cold-rolled specimens were solution-treated for 3.6 ks at 873 K, which is in α single-phase region, and then water quenched. A schematic illustration of the heat treatment procedure for the α single phase is given in Fig. 1. The oxygen contents in all of the alloys were measured using oxygen–nitrogen analyzer (*EMGA-620 W*, *Horiba Japan*).

Microstructures were observed with optical microscope (OM) and scanning electron microscope (SEM) for the specimens finely polished and chemically etched by using a mixture of 5% hydrofluoric acid solution. The SEM (VE9800, KEYENCE Japan) observation was conducted at 15 kV.

The transmission electron microscope (TEM) was also used for detailed microstructure observation. Thin foil specimens for TEM observation (⌀3 mm) were prepared by twin-jet electro polishing in a chemical solution of 60% methanol, 35% butanol and 5% perchloric acid at 243 K. The TEM observation was carried out with JEM-2010EX, JEOL Japan operated at 200 kV. Also, the detailed microstructure and element distribution were investigated by using a scanning transmission electron microscope (STEM) with energy-dispersive X-ray spectroscopy (EDS). Thin foil specimens for STEM with EDS were manufactured in same method with TEM. The STEM with EDS was operated at an accelerating voltage of 200 kV (JEM-ARM 200F, JEOL JAPAN).

The X-ray diffraction (XRD: RINT RAPID, RIGAKU) analysis was performed for identifying the constituent phases and measuring their volume fraction and lattice parameters, by using Co Kα radiation at an accelerating voltage of 40 kV and a current of 30 mA. The specimens for XRD were chemically polished with a water solution containing 60% hydrogen peroxide and 10% hydrofluoric acid. The hcp structural lattice parameters were evaluated using Eq. (1) with the experimentally observed $\sin^2\theta$ [11]:

$$\sin^2\theta-\frac{\lambda^2}{3a^2}(h^2+hk+k^2)-\frac{\lambda^2}{4c^2}(l^2)=D\ \sin^2 2\theta \quad (1)$$

where $\lambda$ is the wave length, *hkl* is the Miller indices of the Bragg plane, *a* and *c* are the lattice parameters of the *hcp* structure, and *D* is the displacement.

The mechanical properties of the prepared alloys were evaluated by Vickers hardness tests, nano-indentation test, and tensile tests at room temperature. The Vickers hardness (*MICROHARDNESS, AKASI Japan*) and the nano-indentation hardness (*ENT-1100A*, *Elionix*) were measured under a 300 gf load and a 2 mN load, respectively.

## 3. Results

### 3.1. Variation in the microstructure of α single-phase Ti alloy with oxygen content

Fig. 2 shows optical micrographs of Ti–0.082, 0.132, 0.197, 0.218 and 0.268 mass% O alloys (hereafter, the mass% is omitted), which were subjected to solution treatment at 873 K for 3.6 ks. It is evident from this that all of these alloys consist of equiaxed grains with an average grain size of about 28–36 μm in diameter.

The XRD patterns obtained from the solution treated Ti–O alloys within a 2-theta angle range of 44–48° as shown in Fig. 3

**Table 1**
Chemical composition of the α single-phase Ti–O alloys used in this study (mass%).

| Alloy | mass% | | | |
|---|---|---|---|---|
| | O | N | H | C |
| Ti–0.082O | 0.082 | 0.009 | 0.007 | 0.004 |
| Ti–0.132O | 0.132 | 0.001 | 0.006 | 0.003 |
| Ti–0.197O | 0.197 | 0.001 | 0.005 | 0.005 |
| Ti–0.218O | 0.218 | 0.001 | 0.006 | 0.004 |
| Ti–0.268O | 0.268 | 0.001 | 0.006 | 0.004 |

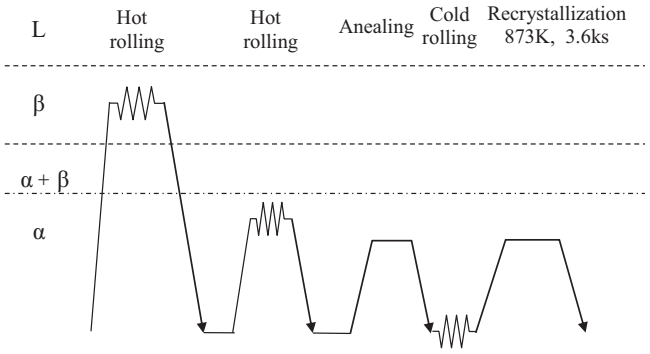


**Fig. 1.** Schematic illustration of the heat treatment procedure for the α single-phase T–O alloys used in this study.

indicate that the phase obtained by solution treatment at 873 K for 3.6 ks is an α phase, with no other precipitates detected. It is observed that the texture is varied depending on oxygen contents. The Ti–0.268O alloy exhibits obvious texture because their strongest peaks are $(0002)_\alpha$ peak rather than $(10\bar{1}1)_\alpha$ peak, which is normally the strongest peak of α phase. Since the intensity of $(0002)_\alpha$ peak is larger than the theoretical diffraction strength ratio ($I_{1010}$:$I_{0002}$:$I_{1011}$=25:30:100), it could be known that texture is developed based on $\langle 0001\rangle_{ND}$ direction during rolling. It is well known that texture in single α phase, which is called as B (basal)-texture, is greatly influenced by alloying elements such as Al and O [12]. This B-texture easily occurred in which the cross rolling is conducted. However, it is unclear why the texture is developed in rolled Ti–O alloy containing large amount of oxygen.

It can also be seen that there is a shift in the diffraction peaks toward a lower angle with increasing oxygen content, which indicates an increase in the lattice parameter. One should note that this shift to lower angles is significantly larger for the $(0002)_\alpha$ peak when compared to the peak shifts of the $(10\bar{1}1)_\alpha$ peak. This means that an octahedral site is favorable to accommodate an oxygen atom as an interstitial, and thus preferentially affected to change the lattice parameter of $(0002)_\alpha$ peak [13]. Given this, the lattice parameters were calculated using not only the $(0002)_\alpha$ and $(10\bar{1}1)_\alpha$ peaks, but also the $(10\bar{1}0)_\alpha$, $(10\bar{1}2)_\alpha$, $(11\bar{2}0)_\alpha$, $(10\bar{1}3)_\alpha$, $(20\bar{2}0)_\alpha$, $(11\bar{2}2)_\alpha$, $(20\bar{2}1)_\alpha$, $(0004)_\alpha$, $(20\bar{2}2)_\alpha$ and $(10\bar{1}4)_\alpha$ peaks.

The variation in lattice parameter as a function of oxygen content is given in Fig. 4, which indicates that the lattice parameters rise with increasing oxygen content. It is therefore evident that oxygen addition expands the crystal lattice of the α phase. However, if we look at the change in lattice parameter in more detail, then it is apparent that the *a* axis varies constantly with increasing oxygen content. Meanwhile, in the Ti–0.082O and Ti–0.132O alloys, the *c* axis exhibits a slight gradual slope that results in a slight increase in the *c*/*a* ratio. In contrast, there is a sharp increase in the *c*/*a* ratio of the Ti–0.197, 0.218 and 0.268O alloys that is brought about by an increase in the *c* axis. It is well known that the ductility of *hcp*-group metals is strongly related to their *c*/*a* ratio, as this determines their slip modes [10]. Consequently, the relationship between *c*/*a* ratio and ductility will be discussed.